

Engineering Notes

ENGINEERING NOTES are short manuscripts describing new developments or important results of a preliminary nature. These Notes cannot exceed 6 manuscript pages and 5 figures; a page of text may be substituted for a figure and vice versa. After informal review by the editors, they may be published within a few months of the date of receipt. Style requirements are the same as for regular contributions (see inside back cover).

Nonlinear Aerodynamic Characteristics of Sounding Rockets

JOHN D. NICOLAIDES,* CHARLES W. INGRAM,† AND
DAVID D. TARKOWSKI‡
University of Notre Dame, Notre Dame, Ind.

Nomenclature

$C_{M\alpha}(\alpha)$	$= M_{\alpha\alpha}/Q S d, \text{ rad}^{-1}$
$C_{M\dot{\alpha}}(\alpha) + C_{M\ddot{\alpha}}(\alpha)$	$= [M_{\dot{\alpha}}(\alpha) + M_{\ddot{\alpha}}(\alpha)]/(Q S d^2/2V), \text{ rad}^{-2}$
$C_{M p\alpha}(\alpha)$	$= M_{p\alpha}(\alpha)/(Q S d^2/2V), \text{ rad}^{-2}$
Re	$= \text{Reynolds number based on length}$
d	$= \text{reference diam, ft}$
S	$= \text{reference area, } \pi d^2/4, \text{ ft}^2$
Q	$= \text{dynamic pressure, lb/ft}^2$
V	$= \text{velocity, fps}$

Introduction

THE two most often encountered instabilities of sounding rockets are Magnus instability and catastrophic yaw.¹ Magnus instability generally results from high roll rates which increase the adverse effect of the Magnus moment on the rocket's damping characteristics. In attempting to avoid Magnus instability by reducing the roll rate, catastrophic yaw may be encountered. Conversely, roll lock-in and catastrophic yaw can usually be avoided, if the configuration is designed to have a steady-state roll rate p greater than the nutation rate ω_n . However at these high-roll rates, Magnus instability usually results. The dynamicist faces a very delicate situation with regard to insuring flight stability of sounding rockets. If the Magnus moment could be controlled or eliminated at the high roll rates, the stability and accuracy of sounding rockets could be assured. One anti-Magnus de-

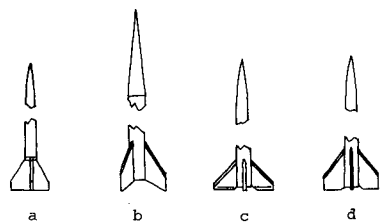


Fig. 1 Army Apache, Black Brandt IIIB, NASA and Sandia Tomahawk sounding rocket configurations analyzed.

Presented as Paper 70-1383 at the AIAA 2nd Sounding Rocket Technology Conference, Williamsburg, Va., December 7-9, 1970; submitted December 3, 1970; revision received July 23, 1971. The authors would like to thank T. A. Clare of the Naval Weapons Laboratory, formerly a graduate student at Notre Dame, for his valuable contributions to this research program. Project supported by NASA Goddard, Sandia Laboratories (AEC), Atmospheric Sciences Laboratory, White Sands, New Mexico, and Raytheon Company.

* Professor, Aerospace and Mechanical Engineering. Associate Fellow Member AIAA.

† Assistant Professor, Aerospace and Mechanical Engineering. Member AIAA.

‡ Research Assistant, Aerospace and Mechanical Engineering. Associate Member AIAA; currently 2nd Lt., U.S. Army Missile Systems Command, Redstone Arsenal, Ala.

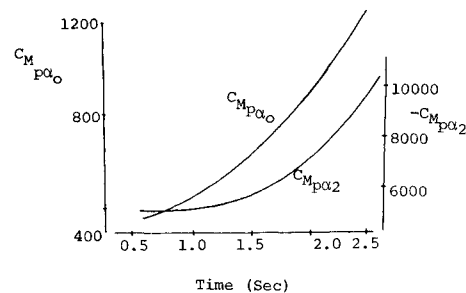


Fig. 2 $C_{Mp\alpha_0}$ and $C_{Mp\alpha_2}$ vs time.

vice, fin tabs, has proven to be effective on an Apache model in three-degrees-of-freedom dynamic wind-tunnel tests. The results of this investigation are presented herein.

Within the last three years, advanced research dynamics^{2,3} has led to the formulation and application of a nonlinear aeroballistic theory, which, combined with the wobble computer program,⁴ has been successfully fitted to constrained single and three-degrees-of-freedom wind-tunnel data, and both full-scale and free-flight, wind-tunnel data.

This Note presents the stability coefficients determined from free-flight data, for four sounding rockets, the NASA Tomahawk, Army Apache, Sandia Tomahawk, and Black Brandt IIIB. The wobble computer program was used to fit short segments of data in overlapping sections, so that the stability parameters could be determined as functions of time. Application of the nonlinear theory yields the restoring, damping, and Magnus stability coefficients as polynomial functions of angle of attack:

$$C_{M\alpha}(|\alpha|) = C_{M\alpha_0} + C_{M\alpha_2}|\alpha|^2 \quad (1)$$

$$C_{M\dot{\alpha}}(|\alpha|) + C_{M\ddot{\alpha}}(|\alpha|) = (C_{M\dot{\alpha}} + C_{M\ddot{\alpha}})_0 + (C_{M\dot{\alpha}} + C_{M\ddot{\alpha}})_2|\alpha|^2 \quad (2)$$

$$C_{Mp\alpha}(|\alpha|) = C_{Mp\alpha_0} + C_{Mp\alpha_2}|\alpha|^2 \quad (3)$$

If the value of each term for the sectional fit remains relatively constant, then the polynomial is felt to define its nonlinear variations with α . If the values of the terms vary with time, as the Magnus terms did, then a Reynolds number effect is felt to be present and no exact functional relation can be established.

Army Apache

The Apache firings were made in conjunction with the Ballistic Missile Target System being developed by the Raytheon Co. The Apache is the second stage of the Nike-Apache vehicle and is shown in Fig. 1a. The nominal mass parameters are shown in Table 1. The data from the three free-flight tests, furnished by the Raytheon Company, and two free-flight wind-tunnel tests, furnished by Arnold Research Organization, were analyzed and found to be in good agreement

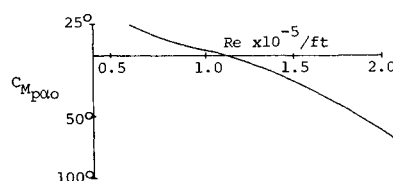


Fig. 3 $C_{Mp\alpha_0}$ vs Re .

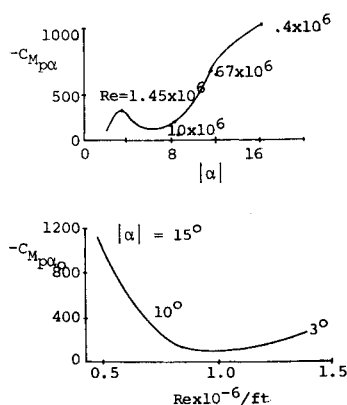


Fig. 4 C_{Mpa} vs $|\alpha|$ and Re .

for C_{Ma0} (Table 1) from all tests. From the free-flight full-scale data analysis $C_{Mpa} = 561$ was obtained. Because of the poor resolution of the data, $C_{Mq}(|\alpha|) + C_{M\dot{\alpha}}(|\alpha|)$ and the nonlinear terms $C_{Ma2}(C_{Mq} + C_{M\dot{\alpha}})_2$ and C_{Mpa2} could not be determined.

Black Brandt IIIB

The Black Brandt IIIB is a single-stage, three-finned vehicle (Fig. 1b and Table 1). Angular data from a portion of the re-entry flight were analyzed. The angular motion was obtained by gyro telemetry from a roll-stabilized platform and the trajectory data were obtained from radar output. $C_{Ma}(|\alpha|)$ in Eq. (1) (Table 1) determined from this flight was found to be a hard spring restoring moment.

The damping moment coefficient approached zero as $|\alpha|$ approached 20° , indicating that a damping instability would result at $|\alpha| > 20^\circ$. From the wobble fits C_{Mpa} was found to go from a negative to a positive value. Upon calculating the linear and nonlinear terms of $C_{Mpa}(|\alpha|)$ in Eq. (3), a time variation was seen (Fig. 2). Cross-plotting these data against α and Re (Fig. 3) does not show a clear dependence on either. Thus, it was felt that the Magnus coefficient was reflecting the combined effects of Re and α . In order to completely establish these functional relationships additional flights would be required.

NASA Tomahawk

The NASA Tomahawk is a single-stage cruciform-finned rocket (Fig. 1c and Table 1). It differs from the Sandia Tomahawk in its over-all length, nose shape, and fin size and

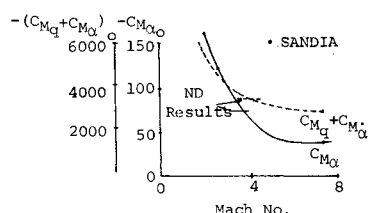


Fig. 5 C_{Ma0} and $(C_{Mq} + C_{M\dot{\alpha}})_0$ vs Mach No. compared with Sandia wind-tunnel tests.

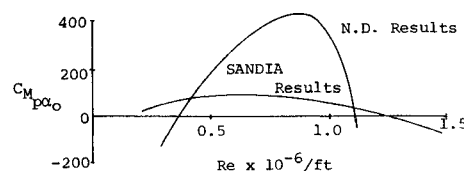


Fig. 6 C_{Mpa0} vs Re compared with Sandia free-flight analysis.

shape. The free-flight analysis was made on a portion of a re-entry flight. The angular motion and trajectory data were obtained from gyro telemetry and radar tracking, which were provided by NASA's Goddard Space Flight Center. The wobble analysis of the angular data detected a precession instability in this flight.

The nonlinearity of the restoring and damping stability coefficients is shown in Table 1. Comparison of C_{Ma0} with tunnel data indicated that good agreement was obtained. The nonlinear variation of $C_{Mq} + C_{M\dot{\alpha}}$ with $|\alpha|$ shows that the damping moment becomes positive at $\alpha = 25^\circ$. Figure 4 presents C_{Mpa} as a function of Re with α as a parameter and as a function of $|\alpha|$ with Re as a parameter. These results were obtained from the analysis of data from only one free-flight test, hence the explicit dependence of the Magnus stability coefficient on Re or α could not be established. The negative value of C_{Mpa} , along with the small values of $C_{Mq} + C_{M\dot{\alpha}}$ at high angles of attack, is the cause for the precession instability observed in the flight data.

Sandia Tomahawk

The Sandia Tomahawk is a single-stage free-flight, cruciform-finned rocket (Fig. 1d and Table 1). The angular and position data analyzed were supplied by the Sandia Corporation and were obtained from gyro telemetry and radar tracking for a re-entry flight. The nonlinearity of $C_{Ma}(|\alpha|)$ and $C_{Mq}(|\alpha|) + C_{M\dot{\alpha}}(|\alpha|)$ are given in Table 1. This data shows that both stability coefficients have a hard spring character.

C_{Ma0} and $(C_{Mq} + C_{M\dot{\alpha}})_0$ as a function of Mach number from Sandia's wind-tunnel test are compared with the results of this analysis in Fig. 5. This comparison is made for low α and the agreement is seen to be quite good. Figure 6 shows C_{Mpa0} for the present results compared with an earlier Sandia free-flight data analysis.⁶ It can be seen that the general variation of C_{Mpa} with Re compares favorably.

Anti-Magnus Device

It was found that fin tabs used as a roll driving mechanism also had a profound effect on the Magnus characteristics of the Apache in wind-tunnel tests.³ These tests indicated that the Magnus stability coefficient would change sign depending on the location of the tabs on the fin. Dynamic three-degree-of-freedom subsonic wind-tunnel tests were conducted for tabs located at outboard and inboard fin positions (Fig. 7). The nonlinear stability coefficients for these tests are shown in Fig. 7. As seen in these results, the nonlinear nature of $C_{Ma}(|\alpha|)$ remained the same. A small reduction in magnitude occurred for the tab inboard since greater tab deflection was required to maintain a constant roll rate, thus reducing fin

Table 1 Mass parameters and stability coefficients for the sounding rockets configuration analyzed

Configuration	Mass, slugs	Length, ft.	Diameter, ft.	Inertia axial transverse, slug/ft ²	C_{Ma0} , rad ⁻¹	C_{Ma2} , rad ⁻³	$(C_{Mq} + C_{M\dot{\alpha}})_0$, rad ⁻¹	$(C_{Mq} + C_{M\dot{\alpha}})_2$, rad ⁻²
Apache	6.56	13.47	0.54	0.65 142.8	-43.3
Black Brandt IIIB	7.90	17.88	0.85	1.16 231.0	-56.0	-56.0	-25,000	200,000
NASA Tomahawk	7.00	16.20	0.75	1.43 201.4	-40.0	-200.0	-3800	20,000
Sandia Tomahawk	8.30	17.50	0.75	1.96 335.0	-80.0	-450.0	-3000	-100,000

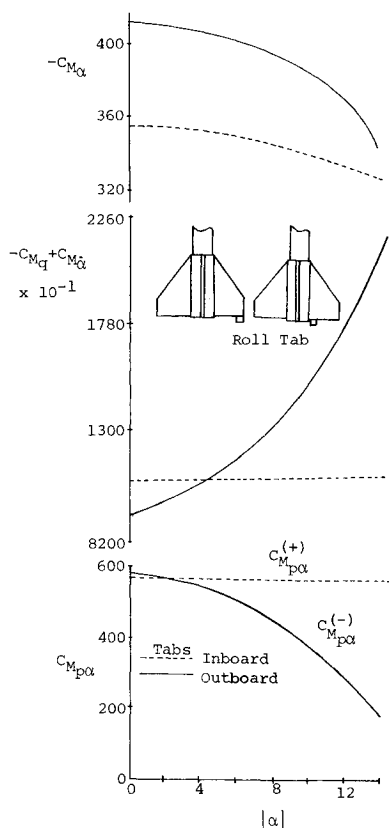


Fig. 7 $C_{M\alpha}$, $C_{Mq} + C_{M\dot{\alpha}}$ and $C_{M_{pa}}$ vs $|\alpha|$ for two roll tab positions.

surface. $C_{Mq}(|\alpha|) + C_{M\dot{\alpha}}(|\alpha|)$ and $C_{M_{pa}}(|\alpha|)$ were found to have drastic alterations of their nonlinear character, as well as the sign of the Magnus stability coefficient being changed. These wind-tunnel tests have shown that fin tabs can be employed as anti-Magnus devices to change the Magnus characteristics of sounding rockets.

Conclusions

This Note has presented $C_{M\alpha}(|\alpha|)$, $C_{Mq}(|\alpha|) + C_{M\dot{\alpha}}(|\alpha|)$ and $C_{M_{pa}}(|\alpha|)$ for the NASA Tomahawk, Sandia Tomahawk, Blackbrandt IIIB, and Army Apache determined from analysis of free-flight data. All stability coefficients were found to be nonlinear functions of $|\alpha|$. However, $C_{M_{pa}}$ was found to be highly nonlinear function of both α and Re . The concept of an Anti-Magnus device for eliminating Magnus instability in fast spinning sounding rockets was demonstrated.

References

- ¹ Nicolaides, J. D., *Free-Flight Dynamics*, Text, Aerospace and Mechanical Engineering Dept. Univ. of Notre Dame, Notre Dame, Ind., 1961, pp. 206-215.
- ² Nicolaides, J. D., Ingram, C. W., and Clare, T. A., "Investigation of the Nonlinear Flight Dynamics of Ordnance Weapons," *AIAA Journal*, Vol. 7, No. 10, Oct. 1970, pp. 1241-1243.
- ³ Ingram, C. W., "On Obtaining the Nonlinear Aerodynamic Stability Coefficients from the Free-Angular Motion of Rigid Bodies," Ph.D. thesis, June, 1969, Aerospace and Mechanical Engineering Dept. Univ. of Notre Dame, Notre Dame, Ind.
- ⁴ Eikenberry, R. S., "Analysis of the Angular Motion of Missiles," SC-CR-70-6051, Feb 1970, Sandia Labs., Albuquerque, N. Mex.
- ⁵ Curry, W. H. and Reed, J. F., "Measurement of Magnus Effects on a Sounding Rocket Model in a Supersonic Wind-Tunnel," AIAA Paper 66-754, Albuquerque, N. Mex., 1966.
- ⁶ Stone, G. W., "The Magnus Instability of a Sounding Rocket," AIAA Paper 66-62, Albuquerque, N. Mex., 1966.

Rapid Technique for Thermal Analysis of PCB Modules

THOMAS M. ZAPPULA*

General Electric Ordnance Systems, Pittsfield, Mass.

Introduction

THE objective is to provide a simple, fast and reliable method for analyzing the thermal characteristics of individual Printed Circuit Boards (PCB). The problem is intensified because the basic external package remains constant while the Printed Circuit Board, a major thermal path and one extremely difficult to define, varies with each one of a large quantity of module designs. This condition is prevalent on any module using the single- or double-sided printed circuit board mounted in a die-cast aluminum frame (Fig. 1).

The thermal resistance through the PCB changes for each module design because of the random location of copper runs, heat-sink copper, and power-dissipating components. Because of these factors, individual theoretical analysis of all but the simplest module construction is tedious, time consuming, and unreliable. While the results of experimental evaluation are the most accurate, it is economically undesirable and impractical to perform experimental evaluation in a reasonable time frame on each module configuration.

The solution was the development of a standard thermal analog matrix with replaceable resistances, a graph of variable resistance values, a table of component interface thermal resistances, and a transparent matrix overlay. A simple and rapid technique was devised through which module thermal characteristics could be obtained in the initial design phases.

Procedure

To obtain a general thermal resistance for each of the three configurations which could then be used in a resistor matrix computer program, a series of experimental tests were conducted using a variety of board configurations. The test boards were divided into a nodal pattern similar to that shown in Fig. 2 and small power resistors were mounted at three of the nodes. Thermocouples were mounted at the power input nodes and at various nodes on the board and the frame. The module assembly was then mounted in a vacuum chamber with only its fin in contact with the base heat sink. Various powers and power-dissipating configurations were then programmed and the nodal temperatures recorded. To keep the information on an easily analyzed level, experiments were conducted on three board configurations—0, 50, and 90%

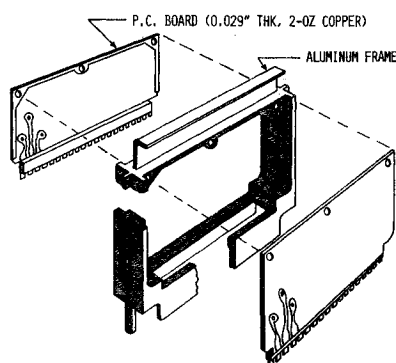


Fig. 1 Typical module configuration.

Received January 16, 1971; revision received July 14, 1971.

Index Category: Launch Vehicle Systems; Launch Vehicle and Missile Subsystem Design; Launch Vehicle and Missile Guidance Systems.

* Product Design Engineer.